

Experimental and Numerical Study of Internal Gear Manufacturing by Flowforming Process and Investigation of Effective Parameters on Teeth Height

Majid Khodadadi

University of Birjand

Khalil Khalili (✉ kkhalili@birjand.ac.ir)

University of Birjand <https://orcid.org/0000-0003-3723-2190>

Amir Ashrafi

University of Birjand

Original Article

Keywords: flowforming, internal gear, finite element analysis, design of experiments, optimization

Posted Date: June 18th, 2020

DOI: <https://doi.org/10.21203/rs.3.rs-36100/v1>

License:   This work is licensed under a Creative Commons Attribution 4.0 International License.

[Read Full License](#)

Abstract

Manufacturing of internal gears using flowforming process is a difficult to achieve but very interesting process in which the gear may be produced without the need for high forming forces and the need for high cost tooling. In this study, manufacturing of internal gears using flowforming process is studied. The process was numerically analyzed and simulated. Several controlled test were performed to evaluate the validity of simulation. A comparison of simulation and experimental results indicates pretty good agreement between these results. Once the simulation is verified, the effects of roller diameter, thickness reduction percentage, feed rate and attack angle on teeth height were obtained using design of experiments (DOE) procedure.

1. Introduction

Flowforming, also known as tube spinning, is a novel metal forming method that is used to produce thin-walled high precision tubular products. A tubular workpiece (preform) is held onto a mandrel, and the material can be displaced axially by one or more rollers moving axially along the mandrel. The advantages of flowforming are flexibility, simple tooling, low production cost and low forming loads, which makes it suitable for automotive industries [1]. Forming a tube along with internal teeth is another application of this process. Gears are generally manufactured using metal cutting processes, which require more time and can lead to material waste. Moreover, gears are subjected to various stress conditions and should be strong enough to withstand these conditions. A gear that is manufactured using a metal cutting procedure has poor strength [2]. To overcome this drawback, flowforming can be used for manufacturing gears.

Because of the importance of flowforming in manufacturing the tubular parts including internal teeth, a number of studies have been carried out through theoretical analyses and experimental methods. Groche and Fritsche [3] investigated gear manufacturing using flowforming. They studied the influence of the number of rollers on the force applied to the mandrel teeth. To achieve a uniform distribution of the force on the mandrel teeth, they suggested using a ring instead of a roller. Jiang et al. [4] studied manufacturing of thin-walled tubes including internal teeth using ball spinning process. They calculated the influence of thickness reduction on teeth height using the finite element method, and compared the results with experiments. Jiang et al. [5] studied the influences of roller diameter, feed rate and the initial thickness of the tube on the height of teeth using neural networks. Jiang et al. [6] simulated manufacturing of thin-walled tubes with internal teeth using finite element method (FEM). They investigated the influence of the roller diameter on teeth height and surface roughness. Jiang et al. [7] investigated the influence of the number of passes during thickness reduction on teeth height, surface roughness and microstructure of the tube. Haghshenas et al. [8] investigated the influences of microstructure, hardness and thickness reduction percentage on the workpiece plastic strain. Haghshenas et al. [9, 10] manufactured internal spline using flowforming and investigated the influence of strain hardening rate on the plastic strain in the metals with fcc structure. Xia et al. [11] analyzed Acme internal gear production defects, experimentally and numerically. The process was applied to Al 6061

using three rollers, and FEM was used to simulate it. Xu et al. [12] studied multi-stage internal gear production using a plate, experimentally and numerically. The process was applied to ASTM 1035 mild steel using three rollers in two stages. Although the process has received attention from the research community, the application of flowforming to manufacture internal gears has been a new attempt so far. The deformation mechanism of teeth in this process is more complex compared with the counterparts with no inner ribs. Moreover, the influence of parameters has not been studied so far.

In the present study, the emphasis is on investigating the influence of process parameters on teeth height in backward flowforming of internal gears using the results of experiment and FEM.

2. Experimental Setup

2.1. Tensile test

To determine the plastic behavior of the material, tensile testing was carried out using the Zwick/Roell tensile test machine with a maximum load of 600 kN and a servo motor control. The setup is shown in Fig. 1. Test samples were prepared according to the ASTM. The tests were carried out with a rate of 20 mm/min at temperatures of 25, 100 and 150°C. The obtained stress-strain diagrams are presented in Fig. 2.

2.2. Friction test

To determine the friction coefficient, the ring pressure test was carried out at temperatures of 25, 60, 100, and 150°C. The test samples were rings with a standard geometric ratio of 2:3:6 (thickness, internal diameter and external diameter of 8, 12 and 24 mm, respectively). A Zwick/Roell pressure test machine with a maximum load of 600 kN was used to carry out the tests (Fig. 3).

2.3. Flowforming process

In this study, a backward flowforming was performed using a universal lathe machine. The preform was a C12200 copper alloy tube with an internal diameter of 13.2 mm and a wall thickness of 2.5 mm (Fig. 4). A ball-bearing (deep groove ball-bearing SKF 6203/VA201 with a diameter of 40 mm and a width of 12 mm) was used as the roller. A gear with 20 teeth and an outer diameter of 13.2 mm, which was heat-treated to get the surface hardness of 58 RC, was used as the mandrel (Fig. 5). The experimental setup is shown in Fig. 6. The gear was complete in four passes of forming. The minimum thickness reduction should be determined so that the plastic metal flow not to be limited to the external surface, which is usually 15% [13]. The primary preform was removed from the mandrel when 25% thickness reduction was achieved. This was repeated in the second step, i.e., another 25% thickness reduction was carried out in the second step. In the third step, the thickness reduction was 20%, and in the fourth step 15%. To evaluate the gear teeth, it was necessary to section the specimens, which was done using a wire-cut

machine. A video measuring machine (VMM) was used to measure the profile and teeth height of gear in the sectioned specimens. Then, the gear microstructure was investigated.

3. Modeling Of Flowforming Process

The model is shown in Fig. 7. In this study, the workpiece material was C12200 copper alloy and considered as an elastic-plastic model (the stress-strain curve is shown in Fig. 2). The mechanical properties of C12200 are shown in Table 1. The geometrical dimensions of pre-form, rollers and mandrel were described in Sect. 2.3. A thermo-mechanical analysis was carried out, and 41470 C3D8RT type elements with the ALE formulation were used for meshing. For simplicity, the mandrel and roller were considered to be rigid. The Coulomb friction model was used to define the contact surfaces, and the friction coefficient was determined according to the friction test (Which was described in Sect. 2.2). Due to high deformation and complicated contact conditions in the flowforming process, the dynamic explicit solving procedure used, because of the numerical robustness and computational efficiency in the case of highly non-linear and large-scale applications[1]. In this analysis, the mass scaling factor was used to reduce the solution time. Finally, to validate the simulation model, the tooth height was compared in two experimental and simulation in four steps, which is shown in Table 2.

Table 1
Mechanical properties of copper workpiece

material	σ_y (MPa)	σ_u (MPa)	E(GPa)	ν	ρ (kg/m ³)
C12200	227	295	115	0.3	8930

Table 2
Comparison between Tooth heights in four steps

	step 1	step 2	step 3	step 4
simulation	0.44	0.84	1.19	1.35
experimental	0.5	0.89	1.21	1.35
error	12%	5%	2%	0

4. Results

4.1. Experimental and simulation results

In this section, the results of simulation and experiments are discussed. The manufacturing of the gear was carried out in four steps and the gear teeth were formed gradually. Figure 8 and Fig. 9 present the form and height of a gear tooth in four steps, which was obtained from the simulation and experimental results.

4.2. Microstructure of gear

Analysis of the microstructure of the gear produced by flowforming helps to understand the deformation mechanism. In this research, samples from the preform and gear (in four passes) were prepared. Microstructures of the samples were obtained by means of a light microscope, and the results are shown in Fig. 10 and Fig. 11. As can be seen in Fig. 10, the microstructure of the preform consists of equiaxed grains, but as shown in Fig. 11, severe deformation and misaligned orientation of the grains in the gear are quite evident, so an inhomogeneous plastic deformation can be inferred. As shown in Fig. 11, the grains are oriented in the tangential and radial directions so that the mandrel grooves are snugly filled. In each pass, the amounts of elongation and deformation of the grains are increased until the fourth pass in which the maximum elongation of the grains is achieved.

4.3. Effective parameters and statistical optimization

Achieving a specific geometry is important in manufacturing industrial components; thus, the investigation of the influence of each parameter on teeth height is necessary. However, there is no concrete objective function to be used by statistical methods for optimizing the process parameters. Response surface method (RSM) was used to investigate the effect of each parameter on teeth height. Response surface method is a statistical method that is used to model and analyze processes that are affected by several parameters. The goal of this method is to model and optimize the response [14]. In this study, a central composite design (CCD) was applied. In this process, four parameters including roller diameter, thickness reduction percentage, feed rate and attack angle (as shown in Fig. 12) are more important than others [1]. The levels of these parameters is given in Table 2 According to the applied method, 31 experiments were considered with $\alpha = 2$.

After doing the tests, the teeth height was obtained for each test, and the ANOVA results were obtained (Table 3). Figure 13 presents the residual distribution of the present study, and the normality of the distribution can be confirmed. A significance level of 95% was selected that the results are correct with a confidence level of 95%. Therefore, a parameter is significant if the P-value is less than 0.05.

According to Table 3, all parameters and interactions are significant and affect the teeth height. Pareto chart is shown in Fig. 14, which expresses the magnitude of the effect of each parameter on teeth height. According to Fig. 14, attack angle (α), thickness reduction percentage (T), interaction between roller diameter and attack angle ($D \times \alpha$), and interaction between roller diameter and feed rate ($D \times f$) are, respectively, the most significant parameters affecting the teeth height. In this analysis, $R-Sq = 99.99$ and $R-Sq (adj) = 99.98$ that confirm ultra-high accuracy of the model developed using RSM. To investigate the influences of the parameters effective on the teeth height, the main effects and interactions should be investigated precisely. In this section, the influence of each parameter will be discussed. In the analysis of interactions, other parameters were considered in a balanced mode (central point) of tests.

Table 2
Effective parameters and their levels

parameter	Roller diameter(D)	Thickness reduction (T %)	Feed rate(f)	Attack angle(α)
Low level	20 mm	15%	0.05 mm/rev	20°
High level	60 mm	35%	0.25 mm/rev	60°

Table 3
ANOVA table for teeth height.

Source	DF	Adj SS	Adj MS	F-Value	P-Value
Model	14	0.345173	0.024655	24023.37	0.000
Linear	4	0.270140	0.067535	65804.28	0.000
D	1	0.000032	0.000032	31.62	0.000
T	1	0.050078	0.050078	48794.72	0.000
f	1	0.002646	0.002646	2577.73	0.000
α	1	0.221872	0.221872	216185.51	0.000
Square	4	0.022202	0.005551	5408.29	0.000
D*D	1	0.000402	0.000402	391.79	0.000
T*T	1	0.008177	0.008177	7967.74	0.000
f*f	1	0.000009	0.000009	8.52	0.011
α * α	1	0.011106	0.011106	10821.19	0.000
2-Way Interaction	6	0.044409	0.007401	7211.73	0.000
D*T	1	0.008587	0.008587	8367.28	0.000
D*f	1	0.011112	0.011112	10827.42	0.000
D* α	1	0.012561	0.012561	12238.90	0.000
T*f	1	0.000686	0.000686	668.81	0.000
T* α	1	0.005527	0.005527	5385.69	0.000
f* α	1	0.000396	0.000396	386.19	0.000
Error	15	0.000015	0.000001		
Lack-of-Fit	9	0.000011	0.000001	1.81	0.242
Pure Error	6	0.000004	0.000001		
Total	29	0.345189			

4.3.1. Influence of roller diameter

The influence of the roller diameter on teeth height is shown in Fig. 15, which indicates that the teeth height increases with increasing the roller diameter up to 40 mm and decreases with further increase. Additionally, according to the $D \times T$ interaction, which is shown in Fig. 16, the height increases with increasing the roller diameter at low thickness reduction percentages, but at values above 25%, the height decreases. As the roller diameter increases, the plastic deformation zone increases, and this leads to an increase in material flow beneath the roller and teeth height. However, as the roller diameter increases (more than 40 mm in Fig. 15 and at thickness reduction values above 25% in Fig. 16), the S/L ratio (circumferential contact length (S) to axial contact length (L)) increases, and due to the friction, the material flow increases in axial direction. However, to increase the gear height, the axial flow must be reduced. According to the $D \times f$ interaction in Fig. 17, the increase in feed rate decreases the teeth height because at high feed rates, the material does not remain beneath the roller and tends to escape from underneath it and flow in the opposite direction of the roller axial movement. However, this effect is reversed by increasing the roller diameter. As the roller diameter increases, the contact area becomes larger and the engagement of roller and the workpiece increases, so the material escape from the roller less frequently. Consequently, increasing the diameter of the roller results in a better flow of materials in the radial direction and an increased teeth height. According to Fig. 18, which shows the $D \times \alpha$ interaction, the teeth height increases with increasing the roller diameter.

4.3.2. Influence of thickness reduction percentage

According to the main effect of thickness reduction percentage (Fig. 19) as well as the interactions of $T \times \alpha$ (Fig. 20) and $D \times T$ (Fig. 16), the teeth height increases with increasing the thickness reduction percentage. As the thickness reduction percentage increases, the plastic deformation zone increases, and this causes an increase in material flow and teeth height. In addition, at high thickness reduction, the S/L ratio decreases and the axial flow is restricted.

4.3.3. Influence of feed rate

According to Fig. 21, increasing the feed rate reduces the teeth height, as described in Subsection 4.1. Increasing feed rate increases the S/L ratio, and due to the friction, the material flow increases in the axial direction and the teeth height decreases. The interaction of $D \times f$ was explained in Subsection 4.1.

4.3.4. Influence of attack angle

The influence of attack angle is shown in Fig. 22, which indicates that the teeth height decreases with increasing the attack angle. This effect can also be seen in Fig. 18 (interaction of $D \times \alpha$) and Fig. 20 (interaction of $T \times \alpha$). If the attack angle is zero, the flow of materials is in the radial direction and increases the gear height. As the attack angle increases, the axial flow of the material also increases, and the gear height decreases.

4.3.4. Response optimization

In the previous sections, the effective parameters on teeth height were found. In this section, we can find the situation for optimizing the response by using response optimization. In fact, in this method, from the selected levels, the best settings are set to achieve the desired goal, which is to achieve maximum teeth height. As shown in Fig. 23, a maximum teeth height of 0.7272 is obtained for $D = 20$ mm, $T = 35\%$, $f = 0.05$ mm/rev and $\alpha = 20^\circ$.

5. Conclusion

In the present study, flowforming process was used to produce an internal gear on a lathe machine. Then, the process was modelled and the model was verified by comparing the simulation and experimental results. Next, the influences of the roller diameter, feed rate, and thickness reduction percentage and attack angle on teeth height were evaluated. Finally, by analyzing the process and obtaining the teeth height for each test, the results of the ANOVA analysis were obtained as follows:

- All parameters and interactions affect teeth height excluding $T \times f$ and $f \times \alpha$ interactions.
- The teeth height initially increases with increasing the roller diameter up to 40 mm, and then, decreases with a further increase in the diameter.
- The teeth height increases with increasing the thickness reduction percentage.
- The teeth height decreases with increasing feed rate.
- The teeth height decreases with increasing the attack angle.
- A maximum teeth height of 0.7272 is obtained for $D = 20$ mm, $T = 35\%$, $f = 0.05$ mm/rev and $\alpha = 20^\circ$.

Declarations

6.1. Availability of data and materials

The datasets used and/or analyzed during the current study are available from the corresponding author on reasonable request.

6.2. Competing interests

The authors declare that they have no competing interests.

6.3. Funding

Not applicable.

6.4. Author's contributions

Khalili designed the work and was a major contributor in data analysis and writing the manuscript. Khodadadi conducted experimental and simulation tests and interpreted the results of the design of experiments (DOE). Ashrafi was instrumental in experimental testing and simulation of process. All authors read and approved the final manuscript.

6.5. Acknowledgements

Not applicable

References

1. C. Wong, T. Dean, and J. Lin, "Incremental forming of solid cylindrical components using flow forming principles," *Journal of Materials Processing Technology*, vol. 153, pp. 60–66, 2004.
2. H. Nägele, H. Wörner, and M. Hirschvogel, "Automotive parts produced by optimizing the process flow forming – machining," *Journal of Materials Processing Technology*, vol. 98, no. 2, pp. 171–175, 2000/01/29/ 2000.
3. P. Groche and D. Fritsche, "Application and modelling of flow forming manufacturing processes for internally geared wheels," *International Journal of Machine Tools and Manufacture*, vol. 46, no. 11, pp. 1261–1265, 2006.
4. S.-Y. Jiang, Z.-Y. Ren, W. Bin, and G.-X. Wu, "General issues of FEM in backward ball spinning of thin-walled tubular part with longitudinal inner ribs," *Transactions of Nonferrous Metals Society of China*, vol. 17, no. 4, pp. 793–798, 2007.
5. S. Jiang, Z. Ren, K. Xue, and C. Li, "Application of BPANN for prediction of backward ball spinning of thin-walled tubular part with longitudinal inner ribs," *Journal of Materials Processing Technology*, vol. 196, no. 1–3, pp. 190–196, 2008.
6. S.-Y. Jiang, Y.-F. Zheng, Z.-Y. Ren, and C.-F. Li, "Multi-pass spinning of thin-walled tubular part with longitudinal inner ribs," *Transactions of Nonferrous Metals Society of China*, vol. 19, no. 1, pp. 215–221, 2009.
7. S. Jiang, Z. Ren, C. Li, and K. Xue, "Role of ball size in backward ball spinning of thin-walled tubular part with longitudinal inner ribs," *Journal of Materials Processing Technology*, vol. 209, no. 4, pp. 2167–2174, 2009.
8. M. Haghshenas, M. Jhaver, R. Klassen, and J. Wood, "Plastic strain distribution during splined-mandrel flow forming," *Materials & Design*, vol. 32, no. 6, pp. 3629–3636, 2011.
9. M. Haghshenas, J. Wood, and R. Klassen, "Investigation of strain-hardening rate on splined mandrel flow forming of 5052 and 6061 aluminum alloys," *Materials Science and Engineering: A*, vol. 532, pp. 287–294, 2012.
10. M. Haghshenas, J. Wood, and R. Klassen, "Effect of strain-hardening rate on the grain-to-grain variability of local plastic strain in spin-formed fcc metals," *Materials Science and Engineering: A*, vol. 552, pp. 376–383, 2012.

11. 11. Q.-X. Xia, L.-Y. Sun, X.-q. Cheng, and B.-Y. Ye, "Analysis of the forming defects of the trapezoidal inner-gear spinning," in *Industrial Engineering and Engineering Management, 2009. IEEM 2009. IEEE International Conference on*, 2009, pp. 2333–2337: IEEE.
12. 12. W. Xu *et al.*, "Numerical simulation and experimental study on multi-pass stagger spinning of internally toothed gear using plate blank," *Journal of Materials Processing Technology*, vol. 229, pp. 450–466, 2016.
13. 13. M. A. Rasouli, A. Taherizadeh, M. Farzin, A. Abdolah, and M. R. Niroomand, "Investigating the effects of process parameters on forming forces and defects formation in tube spinning process of AA6061," *Modares Mechanical Engineering*, vol. 16, no. 12, pp. 186–194, 2017.
14. 14. D. C. Montgomery, *Design and analysis of experiments. 5th ed. New York :John wiley & sons, 2001.*

Figures

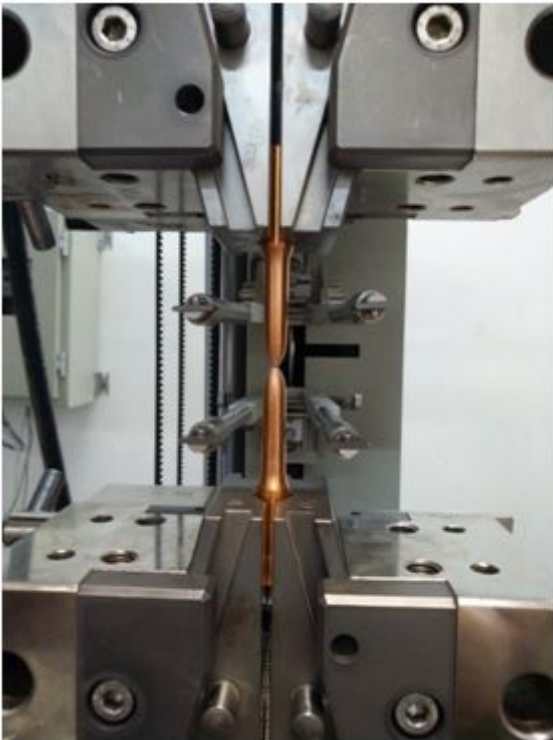


Figure 1

Setup of tensile test equipment.

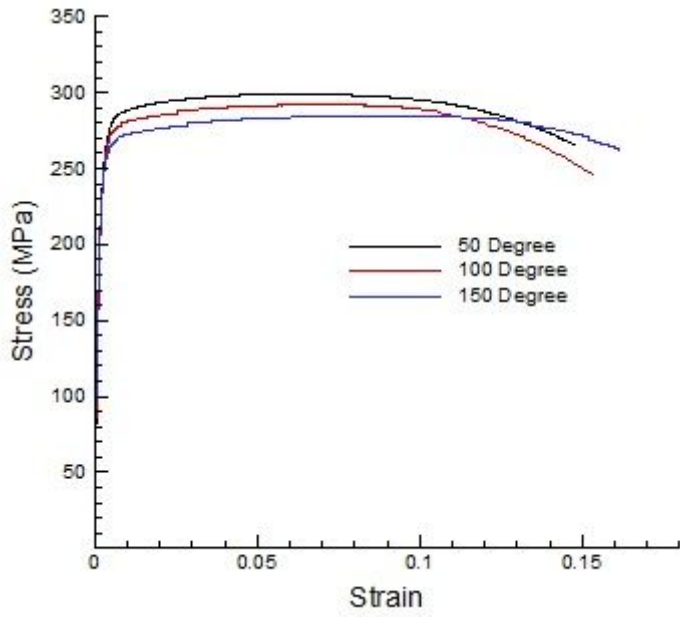


Figure 2

Stress-strain curves of copper workpiece at different temperatures.

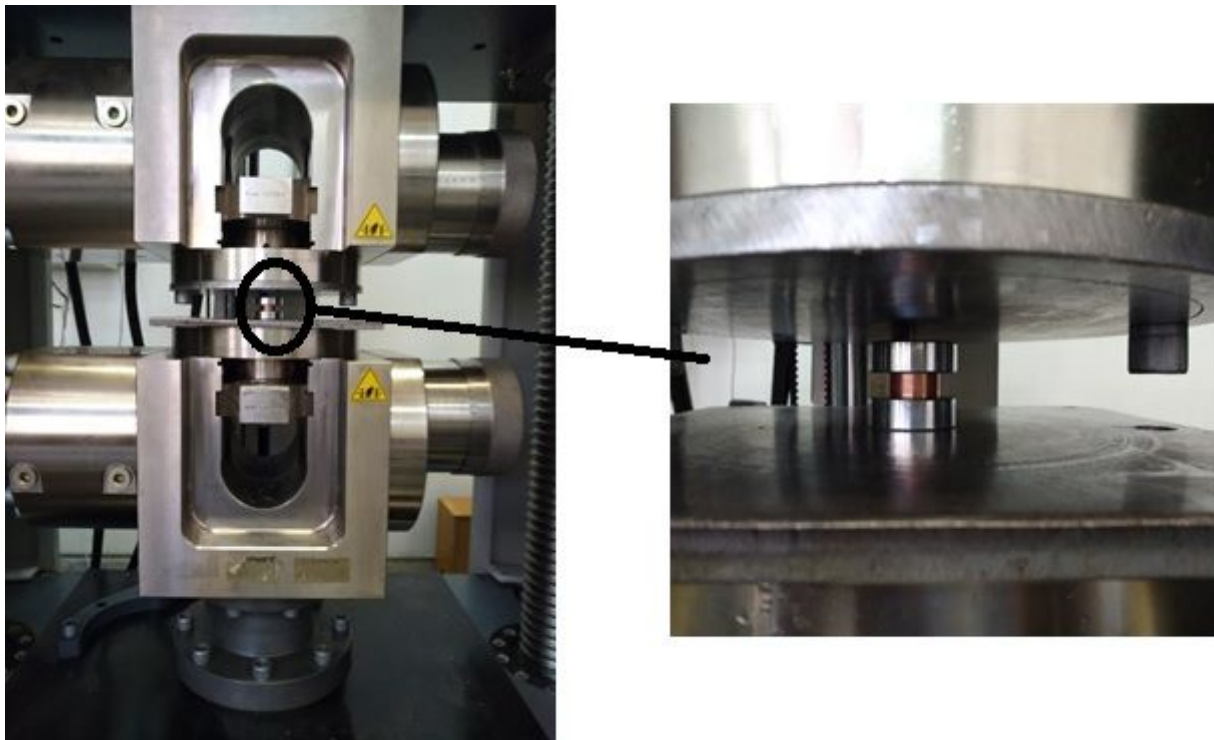


Figure 3

Setup of ring pressure test.

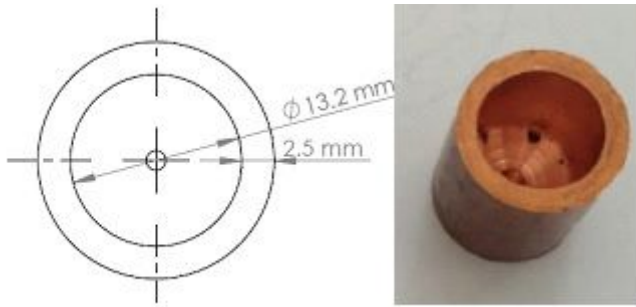


Figure 4

Dimensions of preform.

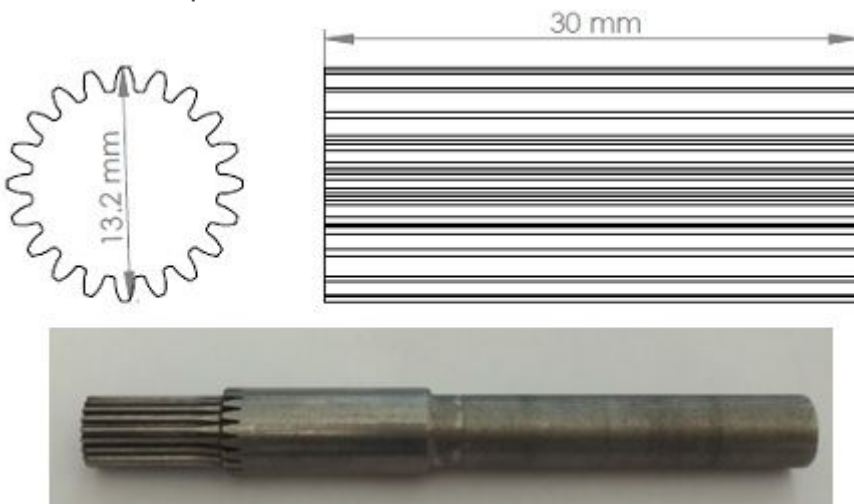


Figure 5

Mandrel used to form internal gear.

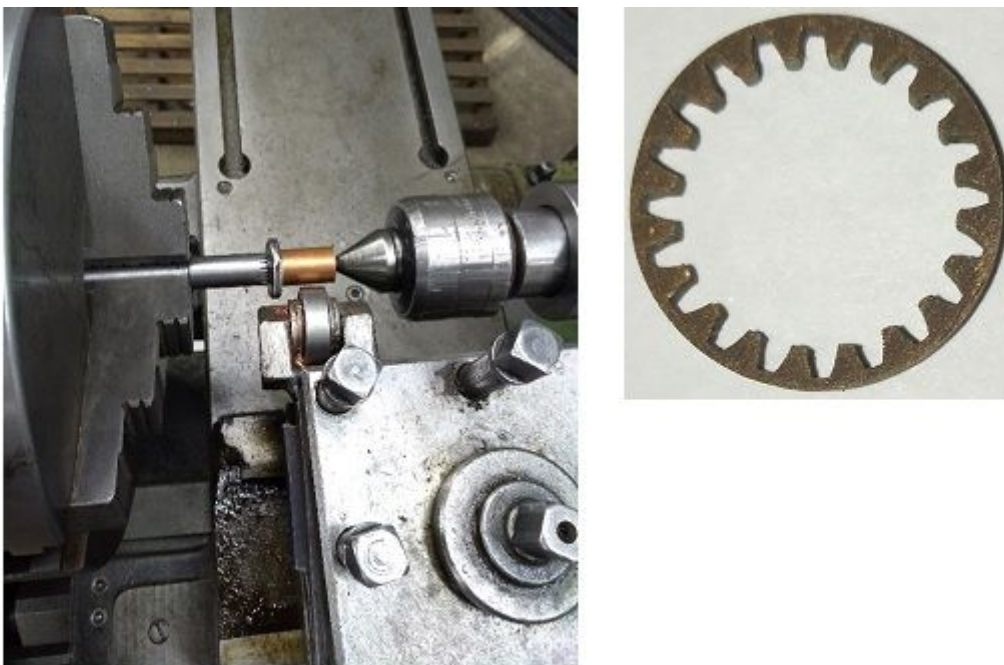


Figure 6

Setup of the experiment and the produced final gear.

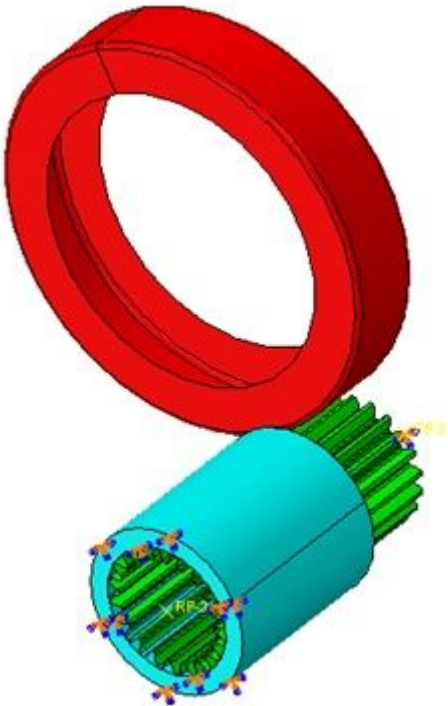


Figure 7

Simulation procedure of flowforming.

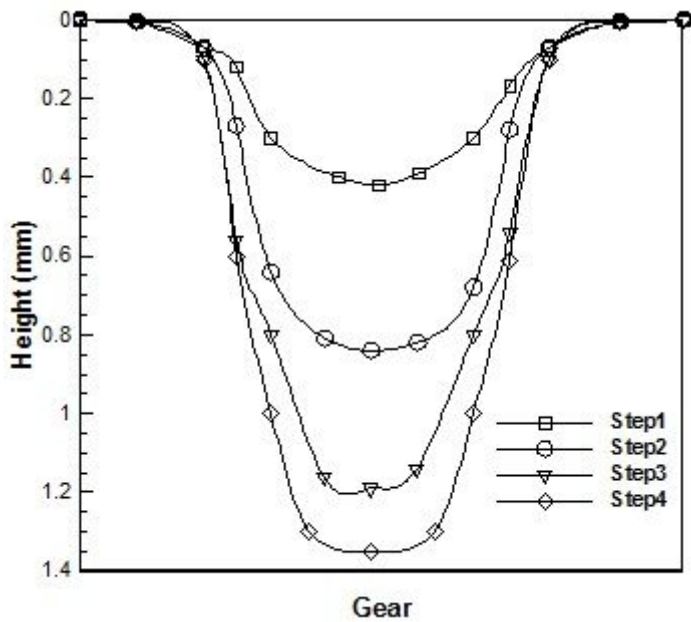


Figure 8

Tooth height at different steps of simulation.

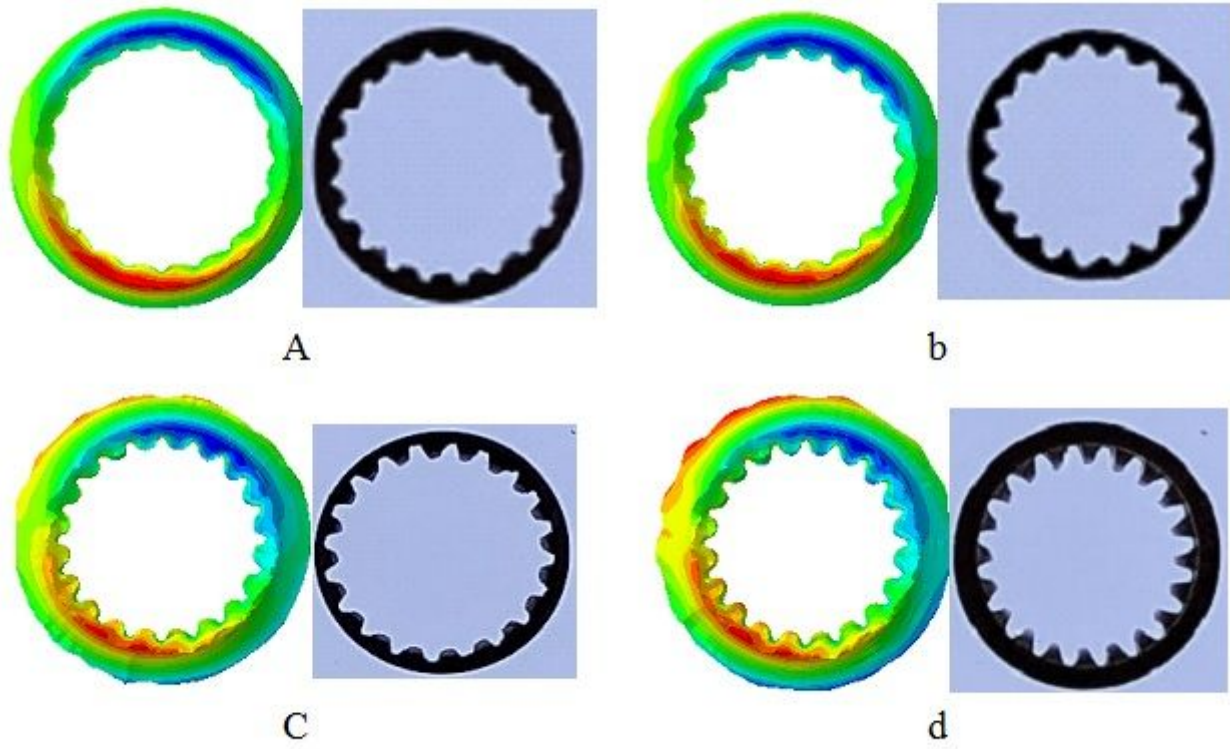


Figure 9

Tooth formation in four steps, a) first step, b) second step, c) third step, and d) fourth step.



Figure 10

Microstructure of preform.

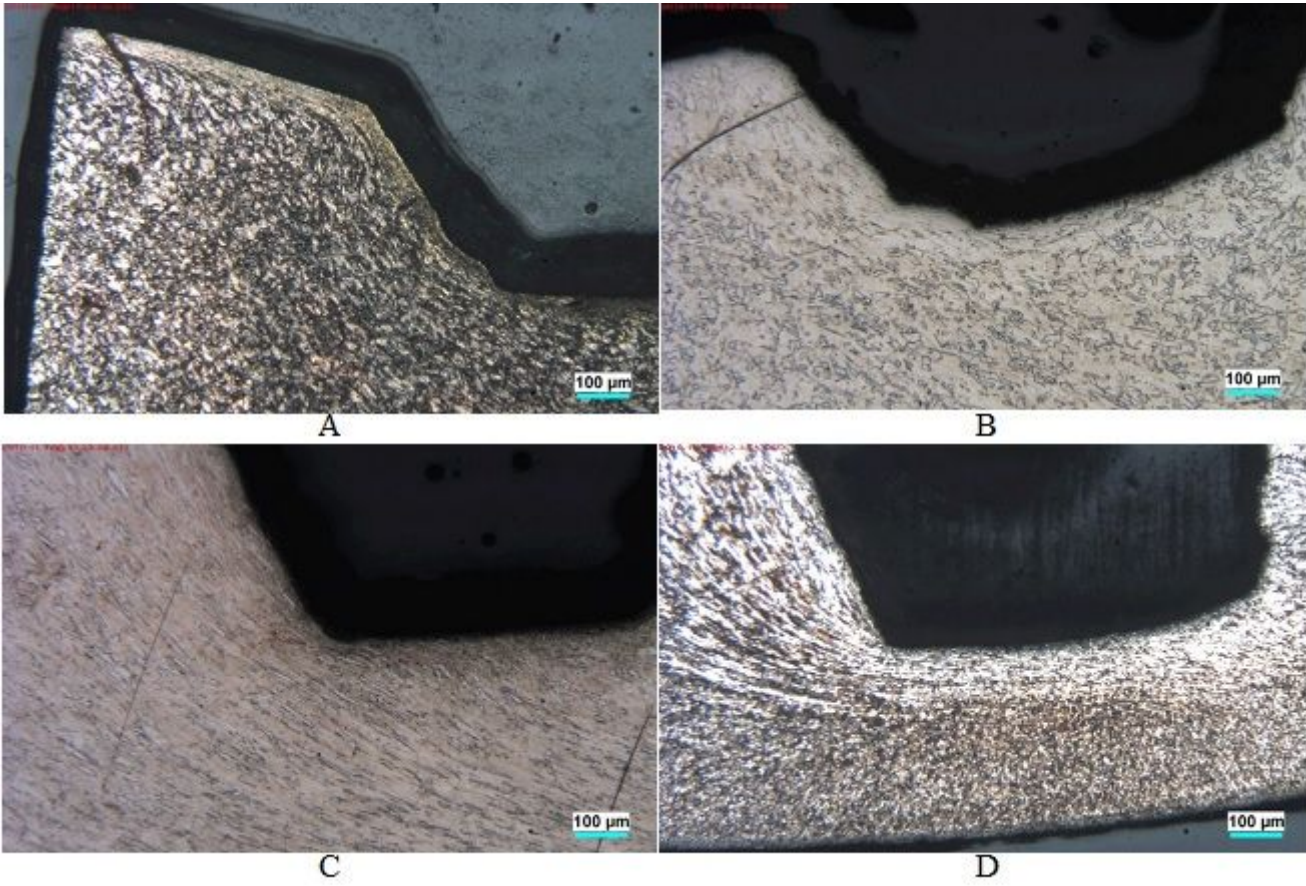


Figure 11

Microstructure of gear, a) Pass1, b) Pass2, c) Pass3 and d) Pass4.

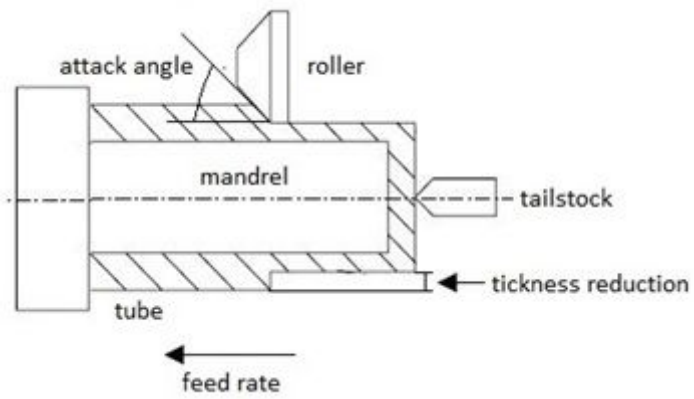


Figure 12

Effective parameters in flowforming process.

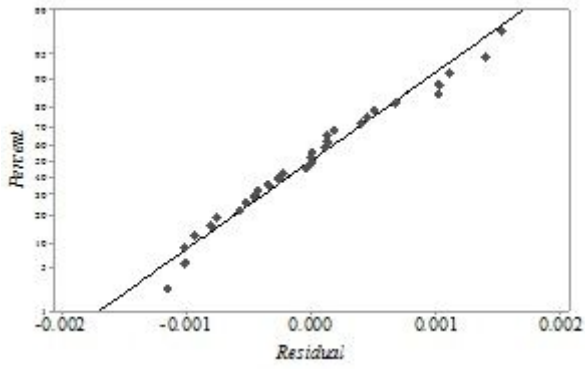


Figure 13

Normal probability of residuals for teeth height.

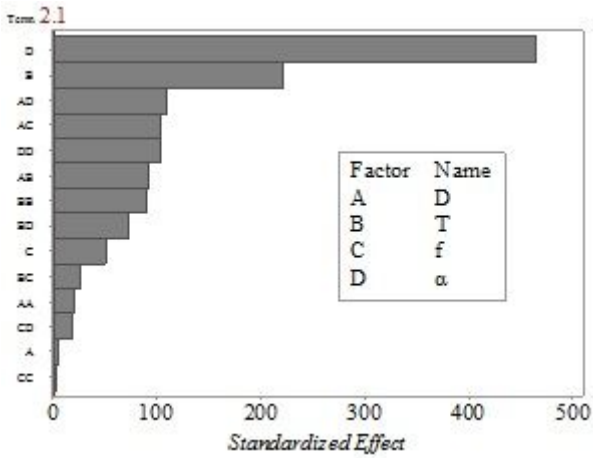


Figure 14

Pareto chart for teeth height.

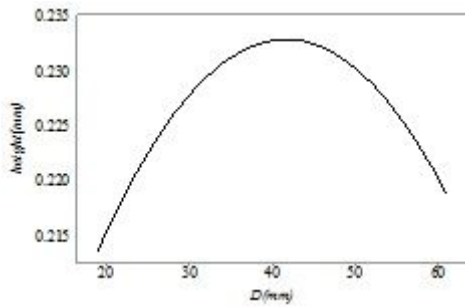


Figure 15

Effect of roller diameter on teeth height.

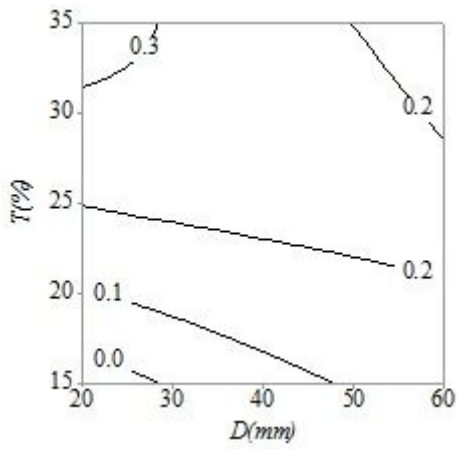


Figure 16

Interaction effects of roller diameter and thickness reduction percentage on teeth height.

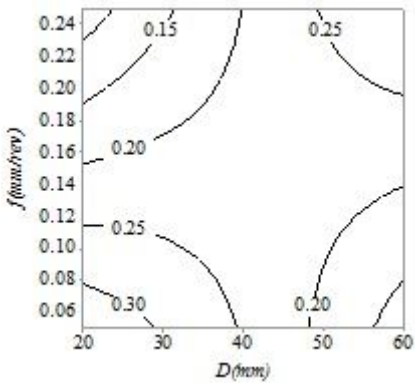


Figure 17

Interaction effects of roller diameter and feed rate on teeth height.

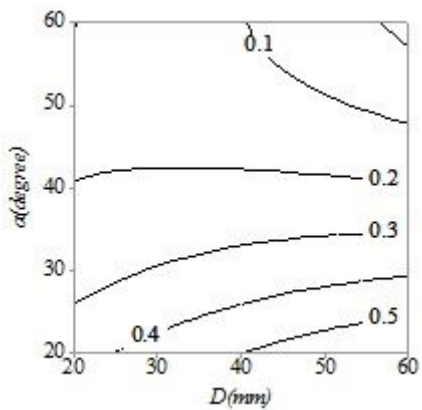


Figure 18

Interaction effects of roller diameter and attack angle on teeth height.

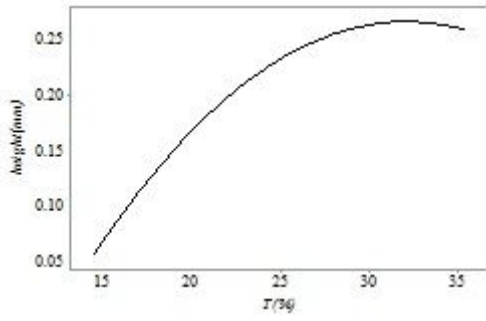


Figure 19

Effect of thickness reduction percentage on teeth height.

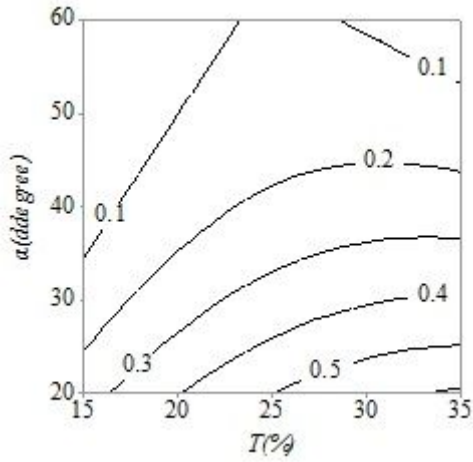


Figure 20

Interaction effects of thickness reduction percentage and attack angle on teeth height.

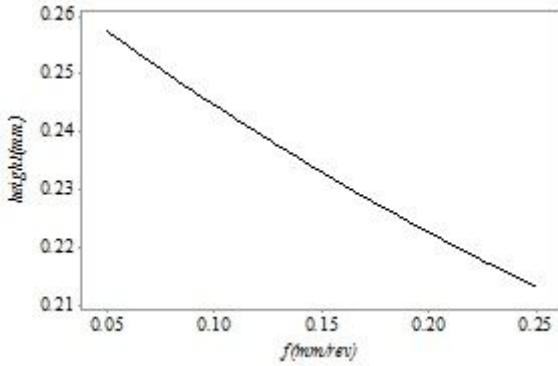


Figure 21

Effect of feed rate on teeth height.

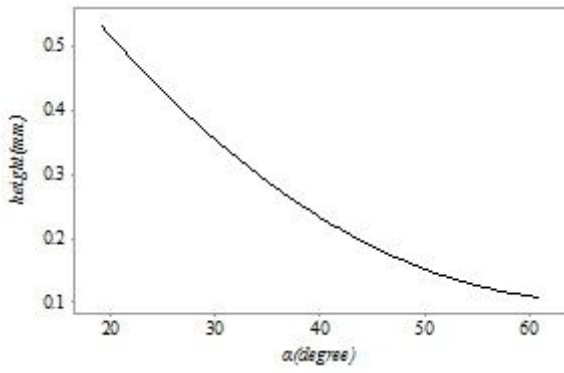


Figure 22

Effect of attack angle on teeth height.

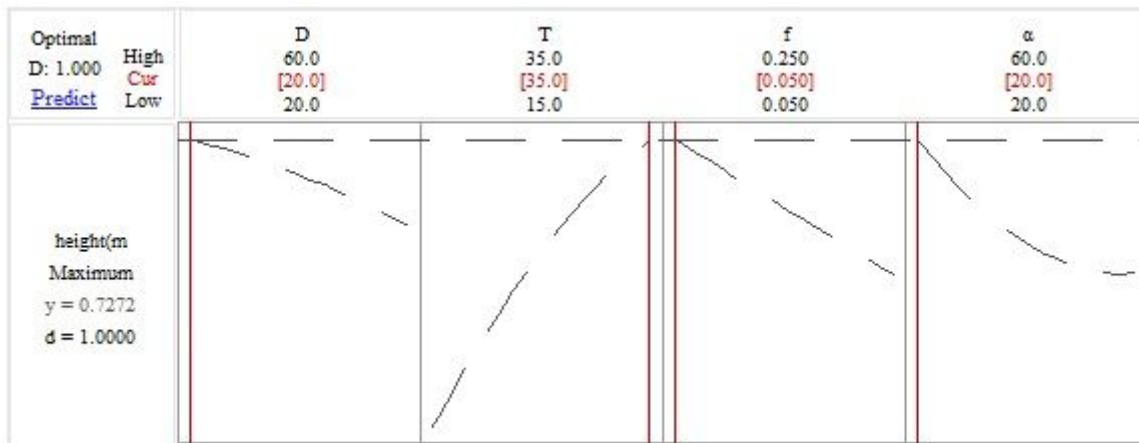


Figure 23

Response optimization plot for teeth height.